










TECH BRIEFS

NATIONAL AERONAUTICS AND SPACE ADMINISTRATION

-  **Technology Focus**
-  **Electronics/Computers**
-  **Software**
-  **Materials**
-  **Mechanics/Machinery**
-  **Manufacturing**
-  **Bio-Medical**
-  **Physical Sciences**
-  **Information Sciences**
-  **Books and Reports**

INTRODUCTION

Tech Briefs are short announcements of innovations originating from research and development activities of the National Aeronautics and Space Administration. They emphasize information considered likely to be transferable across industrial, regional, or disciplinary lines and are issued to encourage commercial application.

Additional Information on NASA Tech Briefs and TSPs

Additional information announced herein may be obtained from the NASA Technical Reports Server: <http://ntrs.nasa.gov>.

Please reference the control numbers appearing at the end of each Tech Brief. Information on NASA's Innovative Partnerships Program (IPP), its documents, and services is available on the World Wide Web at <http://www.ipp.nasa.gov>.

Innovative Partnerships Offices are located at NASA field centers to provide technology-transfer access to industrial users. Inquiries can be made by contacting NASA field centers listed below.

NASA Field Centers and Program Offices

Ames Research Center

Mary Walsh
(650) 604-1405
mary.w.walsh@nasa.gov

Dryden Flight Research Center

Ron Young
(661) 276-3741
ronald.m.young@nasa.gov

Glenn Research Center

Joe Shaw
(216) 977-7135
robert.j.shaw@nasa.gov

Goddard Space Flight Center

Nona Cheeks
(301) 286-5810
nona.k.cheeks@nasa.gov

Jet Propulsion Laboratory

Indrani Graczyk
(818) 354-2241
indrani.graczyk@jpl.nasa.gov

Johnson Space Center

John E. James
(281) 483-3809
john.e.james@nasa.gov

Kennedy Space Center

David R. Makufka
(321) 867-6227
david.r.makufka@nasa.gov

Langley Research Center

Michelle Ferebee
(757) 864-5617
michelle.t.ferebee@nasa.gov

Marshall Space Flight Center

Jim Dowdy
(256) 544-7604
jim.dowdy@nasa.gov

Stennis Space Center

Ramona Travis
(228) 688-3832
ramona.e.travis@ssc.nasa.gov

NASA Headquarters

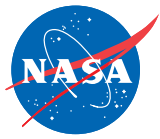
Innovative Partnerships Office

Doug Comstock, Director
(202) 358-2221
doug.comstock@nasa.gov

Daniel Lockney,
Technology Transfer Lead
(202) 358-2037
daniel.p.lockney@nasa.gov

Small Business Innovation Research (SBIR) & Small Business Technology Transfer (STTR) Programs

Carl Ray, Program Executive
(202) 358-4652
carl.g.ray@nasa.gov



TECH BRIEFS

NATIONAL AERONAUTICS AND SPACE ADMINISTRATION



5 Technology Focs: Data Acquisition

- 5 Flight Test Results from the Rake Airflow Gage Experiment on the F-15B
- 5 Telemetry and Science Data Software System
- 6 CropEx Web-Based Agricultural Monitoring and Decision Support
- 6 High-Performance Data Analysis Tools for Sun-Earth Connection Missions
- 7 Experiment in Onboard Synthetic Aperture Radar Data Processing



9 Manufacturing & Prototyping

- 9 Microfabrication of a High-Throughput Nanochannel Delivery/Filtration System
- 9 Improved Design and Fabrication of Hydrated-Salt Pills
- 10 Monolithic Flexure Pre-Stressed Ultrasonic Horns



11 Electronics/Computers

- 11 Cryogenic Quenching Process for Electronic Part Screening
- 11 Broadband Via-Less Microwave Crossover Using Microstrip-CPW Transitions
- 12 Wheel-Based Ice Sensors for Road Vehicles



13 Software

- 13 G-DYN Multibody Dynamics Engine
- 13 Multibody Simulation Software Testbed for Small-Body Exploration and Sampling
- 13 Propulsive Reaction Control System Model
- 13 Licklider Transmission Protocol Implementation
- 14 Core Recursive Hierarchical Image Segmentation



15 Mechanics/Machinery

- 15 Two-Stage Centrifugal Fan
- 15 Combined Structural and Trajectory Control of Variable-Geometry Planetary Entry Systems

- 16 Pressure Regulator With Internal Ejector Circulation Pump, Flow and Pressure Measurement Porting, and Fuel Cell System Integration Options



17 Materials & Coatings

- 17 Temperature-Sensitive Coating Sensor Based on Hematite
- 17 Standardization of a Volumetric Displacement Measurement for Two-Body Abrasion Scratch Test Data Analysis
- 18 Detection of Carbon Monoxide Using Polymer-Carbon Composite Films
- 18 Substituted Quaternary Ammonium Salts Improve Low-Temperature Performance of Double-Layer Capacitors
- 19 Sustainably Sourced, Thermally Resistant, Radiation Hard Biopolymer



21 Physical Sciences

- 21 Integrated Lens Antennas for Multi-Pixel Receivers
- 22 180-GHz Interferometric Imager
- 22 Maturation of Structural Health Management Systems for Solid Rocket Motors
- 22 Validating Phasing and Geometry of Large Focal Plane Arrays
- 23 Transverse Pupil Shifts for Adaptive Optics Non-Common Path Calibration
- 23 Qualification of Fiber Optic Cables for Martian Extreme Temperature Environments
- 24 Solid-State Spectral Light Source System
- 24 Multiple-Event, Single-Photon Counting Imaging Sensor



27 Books & Reports

- 27 Surface Modeling to Support Small-Body Spacecraft Exploration and Proximity Operations
- 27 Achieving Exact and Constant Turnaround Ratio in a DDS-Based Coherent Transponder

This document was prepared under the sponsorship of the National Aeronautics and Space Administration. Neither the United States Government nor any person acting on behalf of the United States Government assumes any liability resulting from the use of the information contained in this document, or warrants that such use will be free from privately owned rights.



Flight Test Results from the Rake Airflow Gage Experiment on the F-15B

The primary goal is to identify the relationship between free stream and local mach number in the low supersonic regime.

Dryden Flight Research Center, Edwards, California

The results are described of the Rake Airflow Gage Experiment (RAGE), which was designed and fabricated to support the flight test of a new supersonic inlet design using Dryden's Propulsion Flight Test Fixture (PFTF) and F-15B testbed airplane (see figure). The PFTF is a unique pylon that was developed for flight-testing propulsion-related experiments such as inlets, nozzles, and combustors over a range of subsonic and supersonic flight conditions.

The objective of the RAGE program was to quantify the local flowfield at the aerodynamic interface plane of the Channeled Centerbody Inlet Experiment (CCIE). The CCIE is a fixed representation of a conceptual mixed-compression supersonic inlet with a translating biconic centerbody. The primary goal of RAGE was to identify the relationship between free-stream and local Mach number in the low supersonic regime, with emphasis on the identification of the particular free-stream Mach number that produced a local Mach number of 1.5. Measurements of the local flow angularity, total pressure distortion, and dynamic pressure over the interface plane were also desired.

The experimental data for the RAGE program were obtained during two separate research flights. During both flights,



The NASA Dryden F-15B research test bed with Propulsion Flight Test Fixture pylon and Rake Airflow Gage Experiment rake during flight test.

local flowfield data were obtained during straight and level acceleration segments out to steady-state test points. The data obtained from the two flights showed small variations in Mach number, flow angularity, and dynamic pressure across the interface plane at all flight conditions. The data show that a free-stream Mach number of 1.65 will produce the desired local Mach number of 1.5 for CCIE. The local total pressure

distortion over the interface plane at this condition was approximately 1.5%. At this condition, there was an average of nearly 2° of downwash over the interface plane. This small amount of downwash is not expected to adversely affect the performance of the CCIE inlet.

This work was done by Michael Frederick and Nalin Ratnayake of Dryden Flight Research Center. Further information is contained in a TSP (see page 1). DRC-009-018

Telemetry and Science Data Software System

Goddard Space Flight Center, Greenbelt, Maryland

The Telemetry and Science Data Software System (TSDSS) was designed to validate the operational health of a spacecraft, ease test verification, assist in debugging system anomalies, and provide trending data and advanced science analysis. In doing so, the system parses, processes, and organizes raw data from the Aquarius instrument both on the ground and while in space. In ad-

dition, it provides a user-friendly telemetry viewer, and an instant push-button test report generator. Existing ground data systems can parse and provide simple data processing, but have limitations in advanced science analysis and instant report generation.

The TSDSS functions as an offline data analysis system during I&T (integration and test) and mission opera-

tions phases. After raw data are downloaded from an instrument, TSDSS ingests the data files, parses, converts telemetry to engineering units, and applies advanced algorithms to produce science level 0, 1, and 2 data products. Meanwhile, it automatically schedules upload of the raw data to a remote server and archives all intermediate and final values in a MySQL database in time

order. All data saved in the system can be straightforwardly retrieved, exported, and migrated.

Using TSDSS's interactive data visualization tool, a user can conveniently choose any combination and mathematical computation of interesting telemetry points from a large range of time periods (life cycle of mission ground data and mission operations testing), and display a graphical and statistical view of the data. With this graphical user inter-

face (GUI), the data queried graphs can be exported and saved in multiple formats. This GUI is especially useful in trending data analysis, debugging anomalies, and advanced data analysis. At the request of the user, mission-specific instrument performance assessment reports can be generated with a simple click of a button on the GUI.

From instrument level to observatory level, the TSDSS has been operating supporting functional and performance

tests and refining system calibration algorithms and coefficients, in sync with the Aquarius/SAC-D spacecraft. At the time of this reporting, it was prepared and set up to perform anomaly investigation for mission operations preceding the Aquarius/SAC-D spacecraft launch on June 10, 2011.

This work was done by Lakesha Bates and Liang Hong of Goddard Space Flight Center. Further information is contained in a TSP (see page 1). GSC-16035-1

➤ CropEx Web-Based Agricultural Monitoring and Decision Support

Changes in crop health are monitored over time.

Stennis Space Center, Mississippi

CropEx is a Web-based agricultural Decision Support System (DSS) that monitors changes in crop health over time. It is designed to be used by a wide range of both public and private organizations, including individual producers and regional government offices with a vested interest in tracking vegetation health. The database and data management system automatically retrieve and ingest data for the area of interest. Another stores results of the processing and supports the DSS. The processing engine will allow server-side analysis of imagery with support for image sub-setting and a set of core raster operations for image classification, creation of vegetation indices, and change detection.

The system includes the Web-based (CropEx) interface, data ingestion system, server-side processing engine, and a database processing engine. It contains a Web-based interface that has multi-tiered security profiles for multiple users. The interface provides the

ability to identify areas of interest to specific users, user profiles, and methods of processing and data types for selected or created areas of interest. A compilation of programs is used to ingest available data into the system, classify that data, profile that data for quality, and make data available for the processing engine immediately upon the data's availability to the system (near real time).

The processing engine consists of methods and algorithms used to process the data in a real-time fashion without copying, storing, or moving the raw data. The engine makes results available to the database processing engine for storage and further manipulation. The database processing engine ingests data from the image processing engine, distills those results into numerical indices, and stores each index for an area of interest. This process happens each time new data is ingested and processed for the area of interest, and upon subsequent database entries, the database processing engine

qualifies each value for each area of interest and conducts a logical processing of results indicating when and where thresholds are exceeded. Reports are provided at regular, operator-determined intervals that include variances from thresholds and links to view raw data for verification, if necessary.

The technology and method of development allow the code base to easily be modified for varied use in the real-time and near-real-time processing environments. In addition, the final product will be demonstrated as a means for rapid draft assessment of imagery.

This work was done by Craig Harvey and Joel Lawhead of Stennis Space Center.

Inquiries concerning rights for its commercial use should be addressed to:

NVision Solutions, Inc.

13131 Hwy 603

Stennis Technology Park, Suite 301

Bay St. Louis, MS 39520

Phone No.: (228) 242-0015

Refer to SSC-00312.

➤ High-Performance Data Analysis Tools for Sun-Earth Connection Missions

Applications include medical image analysis, hyperspectral imaging, wildlife tracking, and sensor data processing.

Goddard Space Flight Center, Greenbelt, Maryland

The data analysis tool of choice for many Sun-Earth Connection missions is the Interactive Data Language (IDL) by ITT VIS. The increasing amount of data produced by these missions and the increasing complexity of image process-

ing algorithms requires access to higher computing power. Parallel computing is a cost-effective way to increase the speed of computation, but algorithms oftentimes have to be modified to take advantage of parallel systems. Enhancing IDL

to work on clusters gives scientists access to increased performance in a familiar programming environment. The goal of this project was to enable IDL applications to benefit from both computing clusters as well as graphics processing

units (GPUs) for accelerating data analysis tasks.

The tool suite developed in this project enables scientists now to solve demanding data analysis problems in IDL that previously required specialized software, and it allows them to be solved orders of magnitude faster than on conventional PCs. The tool suite consists of three components: (1) TaskDL, a software tool that simplifies the creation and management of task farms, collections of tasks that can be processed independently and require only small amounts of data communication; (2)

mpiDL, a tool that allows IDL developers to use the Message Passing Interface (MPI) inside IDL for problems that require large amounts of data to be exchanged among multiple processors; and (3) GPULib, a tool that simplifies the use of GPUs as mathematical co-processors from within IDL.

mpiDL is unique in its support for the full MPI standard and its support of a broad range of MPI implementations. GPULib is unique in enabling users to take advantage of an inexpensive piece of hardware, possibly already installed in their computer, and achieve orders of

magnitude faster execution time for numerically complex algorithms. TaskDL enables the simple setup and management of task farms on compute clusters.

The products developed in this project have the potential to interact, so one can build a cluster of PCs, each equipped with a GPU, and use mpiDL to communicate between the nodes and GPULib to accelerate the computations on each node.

This work was done by Peter Messmer of Tech-X Corporation for Goddard Space Flight Center. Further information is contained in a TSP (see page 1). GSC-15749-1

➤ Experiment in Onboard Synthetic Aperture Radar Data Processing

The algorithm runs in a parallel/multicore environment, and integrates radiation hardening by software (RHBS) self-protection strategies.

Goddard Space Flight Center, Greenbelt, Maryland

Single event upsets (SEUs) are a threat to any computing system running on hardware that has not been physically radiation hardened. In addition to mandating the use of performance-limited, hardened heritage equipment, prior techniques for dealing with the SEU problem often involved hardware-based error detection and correction (EDAC). With limited computing resources, software-based EDAC, or any more elaborate recovery methods, were often not feasible. Synthetic aperture radars (SARs), when operated in the space environment, are interesting due to their relevance to NASAs objectives, but problematic in the sense of producing prodigious amounts of “raw” data. Prior implementations of the SAR data processing algorithm have been too slow, too computationally intensive, and require too much application memory for onboard execution to be a realistic option when using the type of heritage processing technology described above.

This standard C-language implementation of SAR data processing is distributed over many cores of a Tileria Multi-core Processor, and employs novel Radiation Hardening by Software (RHBS) techniques designed to protect the component processes (one per

core) and their shared application memory from the sort of SEUs expected in the space environment. The source code includes calls to Tileria APIs, and a specialized Tileria compiler is required to produce a Tileria executable. The compiled application reads input data describing the position and orientation of a radar platform, as well as its radar-burst data, over time and writes out processed data in a form that is useful for analysis of the radar observations.

The application is capable of recovering from some types of SEU-induced interference with component processes and/or corruption of the shared application memory, and also writes out performance statistics designed to assist in evaluating the effectiveness of the novel RHBS techniques employed. These performance data are useful in identifying, time-stamping, and (indirectly) geo-locating SEU incidents along with the application’s responses.

The tileSAR software distributes the problem of processing SAR data over an “engine” made up of a number of cooperating parallel processes (one per core). This engine is replicated three times within the Tileria processor; always one process per core, and all engines running in parallel. Each engine also in-

cludes an additional scrubbing process (core), and there is one final triple-voting process external to the engines. When distributing the SAR algorithm among the processes of each engine, the usual single-stringed implementation (each sub-task executed in sequence) is replaced with an implementation where independent operations are carried out concurrently by independent processes. Every opportunity for concurrency within this algorithm is exploited, as this dramatically reduces execution time. The result of each engine’s processing is a series of output records. The processes that make up each engine share a single working set of data, collectively called the engine’s “workspace.” The state of each workspace at each synchronization point is expected to be identical to that of the other engines, and reflects the state of progress the engine has made through its execution of the algorithm. The combined effect of scrubbing and triple-voting enables certain types of workspace corruption to be detected and corrected such that processing may continue without interruption or error.

This work was done by Matthew Holland of Goddard Space Flight Center. Further information is contained in a TSP (see page 1). GSC-15757-1



Microfabrication of a High-Throughput Nanochannel Delivery/Filtration System

Lyndon B. Johnson Space Center, Houston, Texas

A microfabrication process is proposed to produce a nanopore membrane for continuous passive drug release to maintain constant drug concentrations in the patient's blood throughout the delivery period. Based on silicon microfabrication technology, the dimensions of the nanochannel area, as well as microchannel area, can be precisely controlled, thus providing a steady, constant drug release rate within an extended time period. The multilayered nanochannel structures extend the limit of release rate range of a single-layer nanochannel system, and allow a wide range of pre-defined porosity to achieve any arbitrary drug release rate using any preferred nanochannel size. This membrane system could also be applied to molecular filtration or isola-

tion. In this case, the nanochannel length can be reduced to the nanofabrication limit, i.e., 10s of nm.

The nanochannel delivery system membrane is composed of a sandwich of a thin top layer, the horizontal nanochannels, and a thicker bottom wafer. The thin top layer houses an array of microchannels that offers the inlet port for diffusing molecules. It also works as a lid for the nanochannels by providing the channels a top surface. The nanochannels are fabricated by a sacrificial layer technique that obtains smooth surfaces and precisely controlled dimensions. The structure of this nanopore membrane is optimized to yield high mechanical strength and high throughput.

This work was done by Mauro Ferrari, Xuewu Liu, Alessandro Grattoni, Daniel Fine, Sharath Hosali, Randi Goodall, Ryan Medema, and Lee Hudson of the University of Texas Health Science Center for Johnson Space Center. For further information, contact the JSC Innovation Partnerships Office at (281) 483-3809.

In accordance with Public Law 96-517, the contractor has elected to retain title to this invention. Inquiries concerning rights for its commercial use should be addressed to:

*Office of Technology Management
The University of Texas Health Science
Center*

*7000 Fannin Street, Suite 720
Houston, TX 77030*

Refer to MSC-24488-1, volume and number of this NASA Tech Briefs issue, and the page number.

Improved Design and Fabrication of Hydrated-Salt Pills

Salt pills for adiabatic-demagnetization refrigerators could be mass-produced.

Goddard Space Flight Center, Greenbelt, Maryland

A high-performance design, and fabrication and growth processes to implement the design, have been devised for encapsulating a hydrated salt in a container that both protects the salt and provides thermal conductance between the salt and the environment surrounding the container. The unitary salt/container structure is known in the art as a salt pill. In the original application of the present design and processes, the salt is, more specifically, a hydrated paramagnetic salt, for use as a refrigerant in a very-low-temperature adiabatic-demagnetization refrigerator (ADR). The design and process can also be applied, with modifications, to other hydrated salts.

Hydrated paramagnetic salts have long been used in ADRs because they have the desired magnetic properties at low temperatures. They also have some properties, disadvantageous for ADRs, that dictate the kind of enclosures in which they must be housed:

- Being hydrated, they lose water if exposed to less than 100-percent relative humidity. Because any dehydration compromises their magnetic properties, salts used in ADRs must be sealed in hermetic containers.
- Because they have relatively poor thermal conductivities in the temperature range of interest (<0.1 K), integral thermal buses are needed as means of efficiently transferring heat to and from the salts during refrigeration cycles. A thermal bus is typically made from a high-thermal-conductivity metal (such as copper or gold), and the salt is configured to make intimate thermal contact with the metal. Commonly in current practice (and in the present design), the thermal bus includes a matrix of wires or rods, and the salt is grown onto this matrix. The density and spacing of the conductors depend on the heat fluxes that must be accommodated during operation.

Because the salt is hydrated, it must be grown from solution onto the matrix, in a container that, immediately after growth, must be hermetically sealed to complete the salt pill. In the present design and fabrication process, the thermal bus is initially fabricated in two pieces: (1) a unitary piece comprising a square array of parallel copper fingers protruding from a copper disk, and (2) a copper cap that can be bolted into thermal contact with an external object. The disk-and-fingers piece is made from a single copper rod by using automated electrical-discharge machining (EDM) to create the gaps between the rods. Prior to EDM, the bolt holes (for subsequent connection to other parts of the ADR) and two access holes (for use in growing the magnetic salt) are machined into the copper rod.

In a single brazing operation, the two copper pieces constituting the thermal bus are joined together, two stainless-steel weldment rings are joined to the

copper (one at each end), and two stainless-steel collars surrounding the access holes are joined to the copper. After brazing, an outer stainless-steel containment tube is welded to the weldment rings. At this point, the salt pill is hermetically sealed except for the collared openings, which are to be welded shut after the salt is grown.

The size and spacing of the copper fingers are set to provide very high thermal conductance to the salt while minimizing complications caused by surface-tension forces on the salt solution during growth of the salt. The salt is grown by use of a continuous-counterflow technique in which saturated solution is pumped into,

and depleted solution is withdrawn from, the salt pill in such a way that crystallites are first nucleated at the bottom, and then salt crystals grow from the bottom upward in a controlled manner until the entire container is filled with salt. The salt solution is circulated by a dual peristaltic pump, using tubes of different sizes for supply and return so that the flow capability for return exceeds that for supply: This is key to ensuring that the saturated solution occupies only a thin layer above the growing salt, ensuring that salt grows only by extending itself rather than by nucleation at random locations throughout the salt pill. Growing the salt in this way ensures that regard-

less of the configuration and thermal conductance of the thermal bus, there is no premature formation of salt in the upper volume of the salt pill. If allowed to occur, such premature formation could trap pockets of solution.

This salt-growth process can yield a high fill fraction (>98 percent). The process can be automated at a high growth rate. The fabrication and salt-growth processes are suitable for mass production of salt pills for ADRs.

This work was done by Peter J. Shirron, Michael J. DiPirro, and Edgar R. Canavan of Goddard Space Flight Center. Further information is contained in a TSP (see page 1). GSC-14873-1

Monolithic Flexure Pre-Stressed Ultrasonic Horns

Flexures are used rather than stress bolts, allowing one to apply pre-load to the piezoelectric material.

NASA's Jet Propulsion Laboratory, Pasadena, California

High-power ultrasonic actuators are generally assembled with a horn, backing, stress bolt, piezoelectric rings, and electrodes. The manufacturing process is complex, expensive, difficult, and time-consuming. The internal stress bolt needs to be insulated and presents a potential internal discharge point, which can decrease actuator life. Also, the introduction of a center hole for the bolt causes many failures, reducing the throughput of the manufactured actuators.

A new design has been developed for producing ultrasonic horn actuators. This design consists of using flexures rather than stress bolts, allowing one to apply pre-load to the piezoelectric material. It also allows one to manufacture them from a single material/plate, rapid prototype them, or make an array in a plate or 3D structure. The actuator is easily assembled, and application of pre-stress greater than 25 MPa was demonstrated.

The horn consists of external flexures that eliminate the need for the conventional stress bolt internal to the

piezoelectric, and reduces the related complexity. The stress bolts are required in existing horns to provide pre-stress on piezoelectric stacks when driven at high power levels. In addition, the manufacturing process benefits from the amenability to produce horn structures with internal cavities. The removal of the pre-stress bolt removes a potential internal electric discharge point in the actuator. In addition, it significantly reduces the chances of mechanical failure in the piezoelectric stacks that result from the hole surface in conventional piezoelectric actuators. The novel features of this disclosure are:

1. A design that can be manufactured from a single piece of metal using EDM, precision machining, or rapid prototyping.
2. Increased electromechanical coupling of the horn actuator.
3. Higher energy density.
4. A monolithic structure of a horn that consists of an external flexure or flex-

ures that can be used to pre-stress a solid piezoelectric structure rather than a bolt, which requires a through hole in the piezoelectric material.

5. A flexure system with low stiffness that accommodates mechanical creep with minor reduction in pre-stress.

This work was done by Stewart Sherrit, Xiaoyi Bao, Mircea Badescu, and Yoseph Bar-Cohen of Caltech, and Phillip Grant Allen of Cal Poly Pomona for NASA's Jet Propulsion Laboratory. Further information is contained in a TSP (see page 1).

In accordance with Public Law 96-517, the contractor has elected to retain title to this invention. Inquiries concerning rights for its commercial use should be addressed to:

*Innovative Technology Assets Management
JPL
Mail Stop 202-233
4800 Oak Grove Drive
Pasadena, CA 91109-8099
E-mail: iaoffice@jpl.nasa.gov
Refer to NPO-47610, volume and number of this NASA Tech Briefs issue, and the page number.*



Cryogenic Quenching Process for Electronic Part Screening

This process can be used in medical or industrial application of electronics at cryogenic temperatures.

NASA's Jet Propulsion Laboratory, Pasadena, California

The use of electronic parts at cryogenic temperatures (<-100 °C) for extreme environments is not well controlled or developed from a product quality and reliability point of view. This is in contrast to the very rigorous and well-documented procedures to qualify electronic parts for mission use in the -55 to 125 °C temperature range. A similarly rigorous methodology for screening and evaluating electronic parts needs to be developed so that mission planners can expect the same level of high reliability performance for parts operated at cryogenic temperatures.

A formal methodology for screening and qualifying electronic parts at cryogenic temperatures has been proposed. The methodology focuses on the base physics of failure of the devices at cryogenic temperatures. All electronic part reliability is based on the "bathtub" curve, high amounts of initial failures (infant mortals), a long period of nor-

mal use (random failures), and then an increasing number of failures (end of life). Unique to this is the development of custom screening procedures to eliminate early failures at cold temperatures. The ability to screen out defects will specifically impact reliability at cold temperatures.

Cryogenic reliability is limited by electron trap creation in the oxide and defect sites at conductor interfaces. Non-uniform conduction processes due to process marginalities will be magnified at cryogenic temperatures. Carrier mobilities change by orders of magnitude at cryogenic temperatures, significantly enhancing the effects of electric field. Marginal contacts, impurities in oxides, and defects in conductor/conductor interfaces can all be magnified at low temperatures.

The novelty is the use of an ultra-low-temperature, short-duration quenching process for defect screening. The quenching process is designed to identify those defects that will precisely

(and negatively) affect long-term, cryogenic part operation. This quenching process occurs at a temperature that is at least 25 °C colder than the coldest expected operating temperature. This quenching process is the opposite of the standard "burn-in" procedure. Normal burn-in raises the temperature (and voltage) to activate quickly any possible manufacturing defects remaining in the device that were not already rejected at a functional test step. The proposed "inverse burn-in" or quenching process is custom-tailored to the electronic device being used. The doping profiles, materials, minimum dimensions, interfaces, and thermal expansion coefficients are all taken into account in determining the ramp rate, dwell time, and temperature.

This work was done by Douglas J. Sheldon of Caltech and John Cressler of Georgia Tech University for NASA's Jet Propulsion Laboratory. For more information, contact iaoffice@jpl.nasa.gov. NPO-47933

Broadband Via-Less Microwave Crossover Using Microstrip-CPW Transitions

Potential applications include high-frequency probe interfaces, phased-array antennas, and beam-forming networks.

Goddard Space Flight Center, Greenbelt, Maryland

The front-to-back interface between microstrip and CPW (coplanar waveguide) typically requires complex fabrication or has high radiation loss. The microwave crossover typically requires a complex fabrication step. The prior art in microstrip-CPW transition requires a physical vias connection between the microstrip and CPW line on a separate layer. The via-less version of this transition was designed empirically and does not have a close form solution. The prior art of the microwave crossover requires either additional substrate or wire bond as an air bridge to isolate two

microwave lines at the crossing junction. The disadvantages are high radiation loss, no analytical solution to the problem, lengthy simulation time, and complex fabrication procedures to generate air bridges or via. The disadvantage of the prior crossover is a complex fabrication procedure, which also affects the device reliability and yield.

This microstrip-CPW transition is visualized as two microstrip-slotline transitions combined in a way that the radiation from two slotlines cancels each other out. The invention is designed based on analytical methods; thus, it sig-

nificantly reduces the development time. The crossover requires no extra layer to cross two microwave signals and has low radiation loss. The invention is simple to fabricate and design. It produces low radiation loss and can be designed with low insertion loss, with some tradeoff with signal isolation.

The microstrip-CPW transition is used as an interface to connect between the device and the circuit outside the package. The via-less microwave crossover is used to allow two signals to cross without using an extra layer or fabrication processing step to enable this function. This

design allows the solution to be determined entirely through analytical techniques. In addition, a planar via-less microwave crossover using this technique was proposed. The experimental results show that the proposed crossover at 5 GHz has a minimum isolation of 32 dB. It also has low in-band insertion loss and return loss of 1.2 dB and 18 dB, respectively, over more than 44 percent of bandwidth at room temperature.

This microstrip-CPW transition requires the microstrip line to be split into two sections. Each section is connected to a microstrip quarter-wavelength open-ended stub. A slotline is also placed perpendicular to the microstrip section.

The slot is connected to a grounded-end quarter-wavelength slotline and generates a microstrip-slotline transition. When two of these sections are placed in parallel and with the microstrip section combined at transition, a microstrip-CPW transition is formed. The slotline radiation is suppressed as two slots are excited with the electric field in an opposite direction, which cancels the radiation in far field. The invention on the crossover consists of the invented microstrip-CPW transitions combined back-to-back and a microstrip low-pass filter. One signal is crossed through to the microstrip layer, while the other signal is crossed through the CPW line lo-

cated on the ground plane of the microstrip line. The microstrip low-pass filter produces a narrow line at the crossing point to enhance the system isolation. It also produces broadband response in the operating frequency band.

The microstrip-CPW transition allows a microwave signal to travel from microstrip line to CPW line with low radiation loss. The crossover allows two microwave signals to cross with minimal parasitic coupling.

This work was done by Thomas Stevenson, Kongbop U-Yen, Edward Wollack, Samuel Moseley, and Wen-Ting Hsieh of Goddard Space Flight Center. Further information is contained in a TSP (see page 1).GSC-15705-1

Wheel-Based Ice Sensors for Road Vehicles

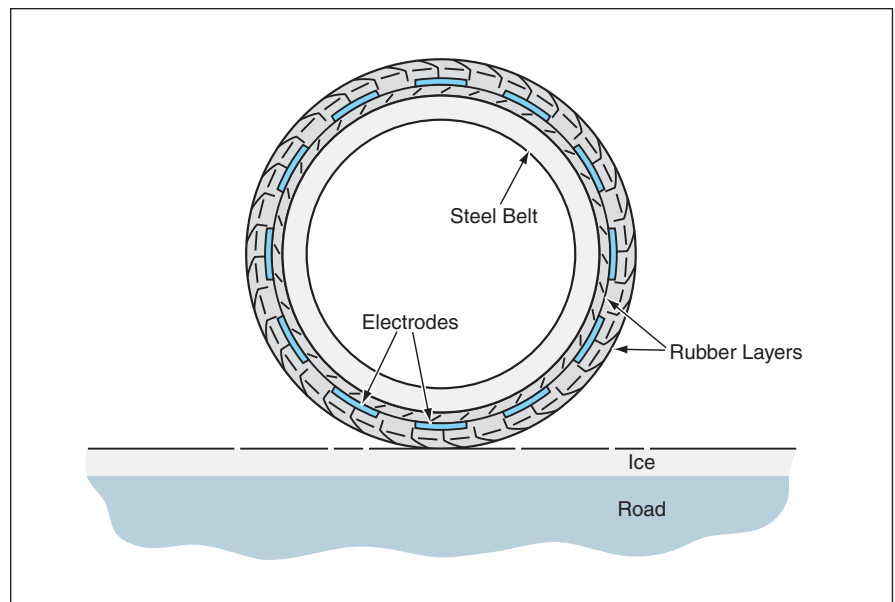
Ice would be sensed via its electric permittivity.

Lyndon B. Johnson Space Center, Houston, Texas

Wheel-based sensors for detection of ice on roads and approximate measurement of the thickness of the ice are under development. These sensors could be used to alert drivers to hazardous local icing conditions in real time. In addition, local ice-thickness measurements by these sensors could serve as guidance for the minimum amount of sand and salt required to be dispensed locally onto road surfaces to ensure safety, thereby helping road crews to utilize their total supplies of sand and salt more efficiently.

Like some aircraft wing-surface ice sensors described in a number of previous *NASA Tech Briefs* articles, the wheel-based ice sensors are based, variously, on measurements of changes in capacitance and/or in radio-frequency impedance as affected by ice on surfaces. In the case of ice on road surfaces, the measurable changes in capacitance and/or impedance are attributable to differences among the electric permittivities of air, ice, water, concrete, and soil. In addition, a related phenomenon that can be useful for distinguishing between ice and water is a specific transition in the permittivity of ice at a temperature-dependent frequency. This feature also provides a continuous calibration of the sensor to allow for changing road conditions.

Several configurations of wheel-based ice sensors are under consideration. For example, in a simple two-electrode capacitor configuration, one of the elec-

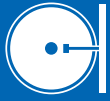


Multiple Electrodes Embedded in a Tire near its outer surface would be excited with alternating voltages. The capacitance between the electrodes at the bottom would be measured as an indication of the thickness of ice (if any) on the road.

trodes would be a circumferential electrode within a tire, and the ground would be used as the second electrode. Optionally, the steel belts that are already standard parts of many tires could be used as the circumferential electrodes. In another example (see figure), multiple electrodes would be embedded in rubber between the steel belt and the outer tire surface. These electrodes would be excited in alternating polarities at one or more suitable audio or radio frequencies to provide nearly con-

tinuous monitoring of the road surface under the tire. In still another example, one or more microwave stripline(s) or coplanar waveguide(s) would be embedded in a tire near its outer surface; in comparison with lower-frequency capacitive devices, a device of this type could be more sensitive.

This work was done by G. Dickey Arndt, Patrick W. Fink, and Phong H. Ngo of Johnson Space Center and James R. Carl (independent consultant). Further information is contained in a TSP (see page 1). MSC-23565-1



G-DYN Multibody Dynamics Engine

G-DYN is a multi-body dynamic simulation software engine that automatically assembles and integrates equations of motion for arbitrarily connected multi-body dynamic systems.

The algorithm behind G-DYN is based on a primal-dual formulation of the dynamics that captures the position and velocity vectors (primal variables) of each body and the interaction forces (dual variables) between bodies, which are particularly useful for control and estimation analysis and synthesis. It also takes full advantage of the sparse matrix structure resulting from the system dynamics to numerically integrate the equations of motion efficiently. Furthermore, the dynamic model for each body can easily be replaced without re-deriving the overall equations of motion, and the assembly of the equations of motion is done automatically.

G-DYN proved an essential software tool in the simulation of spacecraft systems used for small celestial body surface sampling, specifically in simulating touch-and-go (TAG) maneuvers of a robotic sampling system from a comet and asteroid. It is used extensively in validating mission concepts for small body sample return, such as Comet Odyssey and Galahad New Frontiers proposals.

This work was done by Behcet Acikmese, James C. Blackmore, and Milan Mandic of Caltech for NASA's Jet Propulsion Laboratory. For more information, contact iaoffice@jpl.nasa.gov.

This software is available for commercial licensing. Please contact Daniel Broderick of the California Institute of Technology at danielb@caltech.edu. Refer to NPO-47195.

Multibody Simulation Software Testbed for Small-Body Exploration and Sampling

G-TAG is a software tool for the multi-body simulation of a spacecraft with a robotic arm and a sampling mechanism, which performs a touch-and-go (TAG) maneuver for sampling from the surface of a small celestial body. G-TAG utilizes G-DYN, a multi-body simulation engine described in the previous article, and interfaces to controllers, estimators, and

environmental forces that affect the spacecraft. G-TAG can easily be adapted for the analysis of the mission stress cases to support the design of a TAG system, as well as for comprehensive Monte Carlo simulations to analyze and evaluate a particular TAG system design.

Any future small-body mission will benefit from using G-TAG, which has already been extensively used in Comet Odyssey and Galahad Asteroid New Frontiers proposals.

This work was done by Behcet Acikmese, James C. Blackmore, and Milan Mandic of Caltech for NASA's Jet Propulsion Laboratory. Further information is contained in a TSP (see page 1).

This software is available for commercial licensing. Please contact Daniel Broderick of the California Institute of Technology at danielb@caltech.edu. Refer to NPO-47196.

Propulsive Reaction Control System Model

This software models a propulsive reaction control system (RCS) for guidance, navigation, and control simulation purposes. The model includes the drive electronics, the electromechanical valve dynamics, the combustion dynamics, and thrust. This innovation follows the Mars Science Laboratory entry reaction control system design, and has been created to meet the Mars Science Laboratory (MSL) entry, descent, and landing simulation needs. It has been built to be plug-and-play on multiple MSL testbeds [analysis, Monte Carlo, flight software development, hardware-in-the-loop, and ATLO (assembly, test and launch operations) testbeds].

This RCS model is a C language program. It contains two main functions: the RCS electronics model function that models the RCS FPGA (field-programmable-gate-array) processing and commanding of the RCS valve, and the RCS dynamic model function that models the valve and combustion dynamics. In addition, this software provides support functions to initialize the model states, set parameters, access model telemetry, and access calculated thruster forces.

This work was done by Paul Brugarolas, Linh H. Phan, Frederick Serricchio, and Alejandro M. San Martin of Caltech for NASA's Jet Propulsion Laboratory. For more information, contact iaoffice@jpl.nasa.gov.

This software is available for commercial licensing. Please contact Daniel Broderick of the California Institute of Technology at danielb@caltech.edu. Refer to NPO-46978.

Licklider Transmission Protocol Implementation

This software is an implementation of the Licklider Transmission Protocol (LTP), a communications protocol intended to support the Bundle Protocol in Delay-Tolerant Network (DTN) operations. LTP is designed to provide retransmission-based reliability over links characterized by extremely long message round-trip times and/or frequent interruptions in connectivity. Communication in interplanetary space is the most prominent example of this sort of environment, and LTP is principally aimed at supporting "long-haul" reliable transmission over deep-space RF links.

Like any reliable transport service employing ARQ (Automatic Repeat Requests), LTP is "stateful." In order to assure the reception of a block of data it has sent, LTP must retain for possible retransmission all portions of that block which might not have been received yet. In order to do so, it must keep track of which portions of the block are known to have been received so far, and which are not, together with any additional information needed for purposes of retransmitting part, or all, of the block. Long round-trip times mean substantial delay between the transmission of a block of data and the reception of an acknowledgement from the block's destination, signaling arrival of the block. If LTP postponed transmission of additional blocks of data until it received acknowledgement of the arrival of all prior blocks, valuable opportunities to use what little deep space transmission bandwidth is available would be forever lost.

For this reason, LTP is based in part on a notion of massive state retention. Any number of requested transmission conversations (sessions) may be concurrently "in flight" at various displacements along the link between two LTP engines, and the LTP engines must necessarily retain transmission status and retransmission resources for all of them. Moreover, if any of the data of a given block are lost en route, it will be necessary to retain the state of that transmission during an addi-

tional round trip while the lost data are retransmitted; even multiple retransmission cycles may be necessary.

LTP's possible multiplicity of sessions per association makes it necessary for each segment of application data to include an additional demultiplexing token: a "session ID" that uniquely identifies the session in which the segment was issued and, implicitly, the block of data being conveyed by this session.

This software comprises a prototype implementation developed by Johns Hopkins University APL in cooperation with JPL, together with adaptations that improve the robustness, correctness, and operability of that implementation.

This work was done by Scott C. Burleigh and Chris Krupiarz of JHU/APL for NASA's

Jet Propulsion Laboratory. Further information is contained in a TSP (see page 1).

This software is available for commercial licensing. Please contact Daniel Broderick of the California Institute of Technology at danielb@caltech.edu. Refer to NPO-45208.

Core Recursive Hierarchical Image Segmentation

The Recursive Hierarchical Image Segmentation (RHSEG) software has been repackaged to provide a version of the RHSEG software that is not subject to patent restrictions and that can be released to the general public through NASA GSFC's Open Source release process. Like the Core HSEG Software Package, this Core RHSEG Software

Package also includes a visualization program called HSEGViewer along with a utility program HSEGReader. It also includes an additional utility program called HSEGExtract.

The unique feature of the Core RHSEG package is that it is a repackaging of the RHSEG technology designed to specifically avoid the inclusion of the certain software technology. Unlike the Core HSEG package, it includes the recursive portions of the technology, but does not include processing window artifact elimination technology.

This work was done by James Tilton of Goddard Space Flight Center. For further information, contact the Goddard Innovative Partnerships Office at (301) 286-5810. GSC-15983



Two-Stage Centrifugal Fan

Lyndon B. Johnson Space Center, Houston, Texas

Fan designs are often constrained by envelope, rotational speed, weight, and power. Aerodynamic performance and motor electrical performance are heavily influenced by rotational speed. The fan used in this work is at a practical limit for rotational speed due to motor performance characteristics, and there is no more space available in the packaging for a larger fan. The pressure rise requirements keep growing. The way to ordinarily accommodate a higher DP is to spin faster or grow the fan rotor diameter.

The invention is to put two radially oriented stages on a single disk. Flow enters the first stage from the center; en-

ergy is imparted to the flow in the first stage blades, the flow is redirected some amount opposite to the direction of rotation in the fixed stators, and more energy is imparted to the flow in the second-stage blades.

Without increasing either rotational speed or disk diameter, it is believed that as much as 50 percent more DP can be achieved with this design than with an ordinary, single-stage centrifugal design. This invention is useful primarily for fans having relatively low flow rates with relatively high pressure rise requirements.

This work was done by David Converse of Hamilton Sundstrand for Johnson Space

Center. For further information, contact the JSC Innovation Partnerships Office at (281) 483-3809.

Title to this invention has been waived under the provisions of the National Aeronautics and Space Act (42 U.S.C. 2457(f)) to Hamilton Sundstrand. Inquiries concerning licenses for its commercial development should be addressed to:

*Hamilton Sundstrand
Space Systems International, Inc.
One Hamilton Road
Windsor Locks, CT 06096-1010
Phone No.: (860) 654-6000*

Refer to MSC-24881-1, volume and number of this NASA Tech Briefs issue, and the page number.

Combined Structural and Trajectory Control of Variable-Geometry Planetary Entry Systems

This technique can be applied for use in aircraft and underwater vehicles.

NASA's Jet Propulsion Laboratory, Pasadena, California

Some of the key challenges of planetary entry are to dissipate the large kinetic energy of the entry vehicle and to land with precision. Past missions to Mars were based on unguided entry, where entry vehicles carried payloads of less than 0.6 T and landed within 100 km of the designated target. The Mars Science Laboratory (MSL) is expected to carry a mass of almost 1 T to within 20 km of the target site. Guided lifting entry is needed to meet these higher deceleration and targeting demands. If the aerodynamic characteristics of the decelerator are variable during flight, more trajectory options are possible, and can be tailored to specific mission requirements. In addition to the entry trajectory modulation, having variable aerodynamic properties will also favor maneuvering of the vehicle prior to descent. For proper supersonic parachute deployment, the vehicle needs to turn to a lower angle of attack.

One approach to entry trajectory improvement and angle of attack control is to embed a variable geometry decelera-

tor in the design of the vehicle. Variation in geometry enables the vehicle to adjust its aerodynamic performance continuously without additional fuel cost because only electric power is needed for actuating the mechanisms that control the shape change. Novel structural and control concepts have been developed that enable the decelerator to undergo variation in geometry.

Changing the aerodynamic characteristics of a flight vehicle by active means can potentially provide a mechanically simple, affordable, and enabling solution for entry, descent, and landing across a wide range of mission types, sample capture and return, and reentry to Earth, Titan, Venus, or Mars. Unguided ballistic entry is not sufficient to meet this more stringent deceleration, heating, and targeting demands.

Two structural concepts for implementing the cone angle variation, a segmented shell, and a corrugated shell, have been presented. It is possible that a multi-parameter optimization approach will be necessary to fully explore the potential of

the proposed solution. Since the shape of corrugated shell deviates from the conventional sphere-cone decelerator, the variation of aerodynamic characteristics with cone angle obtained is an approximation to that of the corrugated shell decelerator. A more precise numerical computation of the pressure distribution on the corrugated shell surface using panel method is currently underway. This numerical procedure will be incorporated into the trajectory simulation and the structural analysis. Further work will include tuning the current corrugated shell geometry using an energy-based optimization approach to minimize stress and actuation force, and exploring trajectory modulation with decelerators undergoing asymmetric variation in geometry.

Variations in cone angle for a decelerator with sphere-cone geometry have the effect of altering the trim angle of attack and the corresponding lift-to-drag ratio and ballistic coefficients during flight. This capability enables trajectory optimization with fewer aerodynamic constraints. A trajectory simulation with variable aero-

dynamic characteristics demonstrated a reduced deceleration peak and improved landing accuracy. The analytic expressions of the longitudinal aerodynamic coefficients were derived, and guidance laws that track reference heat flux, drag, and aerodynamic acceleration loads are also proposed. These guidance laws, based on dynamic inversion, have been tested in an integrated simulation environment, and

the results indicate that use of variable geometry is feasible to track specific profiles of dynamic and heat load conditions during reentry.

The proposed concept of a decelerator system that is first deployed and then is able to adaptively change its geometry during operation is novel and is expected to lead to reductions of drag up to 20 percent and peak temperature by

20 percent, thus obviating the need for both expensive thermal protection systems and heavy expelled mass ballast to change the aerodynamic configuration of the vehicle.

This work was done by Marco B. Quadrelli, Sergio Pellegrino, and Kawai Kwok of Caltech for NASA's Jet Propulsion Laboratory. Further information is contained in a TSP (see page 1).NPO-47102

Pressure Regulator With Internal Ejector Circulation Pump, Flow and Pressure Measurement Porting, and Fuel Cell System Integration Options

Potential uses include regenerative and primary fuel cell power systems.

Lyndon B. Johnson Space Center, Houston, Texas

An advanced reactant pressure regulator with an internal ejector reactant circulation pump has been developed to support NASA's future fuel cell power systems needs. These needs include reliable and safe operation in variable-gravity environments, and for exploration activities with both manned and unmanned vehicles. This product was developed for use in Proton Exchange Membrane Fuel Cell (PEMFC) power plant reactant circulation systems, but the design could also be applied to other fuel cell system types, (e.g., solid-oxide or alkaline) or for other gas pressure regulation and circulation needs. The regulator design includes porting for measurement of flow and pressure at key points in the system, and also includes several fuel cell system integration options.

NASA has recognized ejectors as a viable alternative to mechanical pumps for use in spacecraft fuel cell power systems. The ejector motive force is provided by a variable, high-pressure supply gas that travels through the ejector's jet nozzle, whereby the pressure energy of the fluid stream is converted to kinetic energy in the gas jet. The ejector can produce circulation-to-consumption-flow ratios that are relatively high (2-3 times), and this phe-

nomenon can potentially (with proper consideration of the remainder of the fuel cell system's design) be used to provide completely for reactant pre-humidification and product water removal in a fuel cell system.

Specifically, a custom pressure regulator has been developed that includes: (1) an ejector reactant circulation pump (with interchangeable jet nozzles and mixer sections, gas-tight sliding and static seals in required locations, and internal fluid porting for pressure-sensing at the regulator's control elements) and (2) internal fluid porting to allow for flow rate and system pressure measurements. The fluid porting also allows for inclusion of purge, relief, and vacuum-breaker check valves on the regulator assembly. In addition, this regulator could also be used with NASA's advanced non-flow-through fuel cell power systems by simply incorporating a jet nozzle with an appropriate nozzle diameter.

For this advanced regulator and ejector concept, ejector flow and outlet pressure are controlled in a manner similar to an "external-sense" regulator. This control method senses the pressure downstream of the ejector mixer outlet, and uses that signal as the feedback to its internal control valve. As changes in

ejector mixer outlet pressure occur as a result of consumption of gases in the fuel cell stack (or system), the regulator's control elements quickly respond with the variable supply of high-pressure gas to the inlet of the ejector jet nozzle to match the real-time flow needs of the fuel cell stack (or system).

In earlier tests of the regulator and ejector assembly at NASA's test facilities, purposefully selected geometry (ejector jet nozzle and mixer internal diameters), pressure, and flow ranges were tested to gather useful performance data to support the development of design guidelines for fuel cell systems utilizing ejectors for reactant circulation. The results of these tests (and with the particular ranges tested) showed that approximate 10:1 ejector-mixer-to-jet diameter ratios could produce performance (scalable over the range of fuel cell power output of 0.7 to 20 kW) that matched the presumed closed fuel cell circulation requirements of total-to-motive flow ratios of 2.5 to 4.5 at the higher motive flow ranges, and with pressure differences developed as high as about 2.5 psid (≈ 17.2 kPa) with reactant gas circulation.

This work was done by Arturo Vasquez of Johnson Space Center. Further information is contained in a TSP (see page 1).MSC-24731-1



Temperature-Sensitive Coating Sensor Based on Hematite

This inexpensive, robust sensor system enables easier measurement and interpretation for optical detection.

John H. Glenn Research Center, Cleveland, Ohio

A temperature-sensitive coating, based on hematite (iron III oxide), has been developed to measure surface temperature using spectral techniques. The hematite powder is added to a binder that allows the mixture to be painted on the surface of a test specimen. The coating dynamically changes its relative spectral makeup or color with changes in temperature. The color changes from a reddish-brown appearance at room temperature (25 °C) to a black-gray appearance at temperatures around 600 °C. The color change is reversible and repeatable with temperature cycling from low to high and back to low temperatures. Detection of the spectral changes can be recorded by different sensors, including spectrometers, photodiodes, and cameras. Using a-priori information obtained through calibration experiments in known thermal environments, the color change can then be calibrated to yield accurate quantitative temperature information. Temperature information can be obtained at a point, or over an entire surface, depending on the type of equipment used for data acquisition.

Because this innovation uses spectrophotometry principles of operation, rather than the current methods, which

use photoluminescence principles, white light can be used for illumination rather than high-intensity short wavelength excitation. The generation of high-intensity white (or potentially filtered long wavelength light) is much easier, and is used more prevalently for photography and video technologies. In outdoor tests, the Sun can be used for short durations as an illumination source as long as the amplitude remains relatively constant. The reflected light is also much higher in intensity than the emitted light from the inefficient current methods. Having a much brighter surface allows a wider array of detection schemes and devices. Because color change is the principle of operation, the development of high-quality, lower-cost digital cameras can be used for detection, as opposed to the high-cost imagers needed for intensity measurements with the current methods.

Alternative methods of detection are possible to increase the measurement sensitivity. For example, a monochrome camera can be used with an appropriate filter and a radiometric measurement of normalized intensity change that is proportional to the change coating temperature. Using different spectral regions

yields different sensitivities and calibration curves for converting intensity change to temperature units. Alternatively, using a color camera, a ratio of the standard red, green, and blue outputs can be used as a self-referenced change. The blue region (<500 nm) does not change nearly as much as the red region (>575 nm), so a ratio of color intensities will yield a calibrated temperature image.

The new temperature sensor coating is easy to apply, is inexpensive, can contour complex shape surfaces, and can be a global surface measurement system based on spectrophotometry. The color change, or relative intensity change, at different colors makes the optical detection under white light illumination, and associated interpretation, much easier to measure and interpret than in the detection systems of the current methods.

This work was done by Timothy J. Bencic of Glenn Research Center. Further information is contained in a TSP (see page 1).

Inquiries concerning rights for the commercial use of this invention should be addressed to NASA Glenn Research Center, Innovative Partnerships Office, Attn: Steven Fedor, Mail Stop 4-8, 21000 Brookpark Road, Cleveland, Ohio 44135. Refer to LEW-18761-1.

Standardization of a Volumetric Displacement Measurement for Two-Body Abrasion Scratch Test Data Analysis

A more robust method is proposed that takes into account the full three-dimensional profile of the displaced material.

John H. Glenn Research Center, Cleveland, Ohio

A limitation has been identified in the existing test standards used for making controlled, two-body abrasion scratch measurements based solely on the width of the resultant score on the surface of the material. A new, more robust method is proposed for analyzing a surface scratch that takes into account the full three-dimensional profile of the displaced mate-

rial. To accomplish this, a set of four volume-displacement metrics was systematically defined by normalizing the overall surface profile to denote statistically the area of relevance, termed the Zone of Interaction. From this baseline, depth of the trough and height of the plowed material are factored into the overall deformation assessment. Proof-of-concept data were

collected and analyzed to demonstrate the performance of this proposed methodology. This technique takes advantage of advanced imaging capabilities that allow resolution of the scratched surface to be quantified in greater detail than was previously achievable.

When reviewing existing data analysis techniques for conducting two-body

abrasive scratch tests, it was found that the ASTM International Standard G 171 specified a generic metric based only on visually determined scratch width as a way to compare abraded materials. A limitation to this method was identified in that the scratch width is based on optical surface measurements, manually defined by approximating the boundaries, but does not consider the three-dimensional volume of material that was displaced. With large, potentially irregular deformations occurring on softer materials, it becomes unclear where to systematically determine the scratch width. Specifically, surface scratches on different samples may look the same from a top view, resulting in an identical scratch width measurement, but may vary in actual penetration depth and/or plowing deformation. Therefore, two different scratch profiles would be

measured as having identical abrasion properties, although they differ significantly.

With these refined measurements, a wider variety of testing needs can be addressed with greater resolution while using the most appropriate abrasive tip and test material combination for the intended application. The core of this innovation in two-body abrasion research involved scratch testing with ASTM G 171 used as a guideline for determining the number of tests to be conducted. The resultant profiles of each scratch were digitized using an optical interferometer and accompanying software. To accomplish this objective, software code was developed to produce a suite of metrics based on a zero line (ZL) through the scratch, which allowed quantitative definition of the scratch and associated wear metrics.

The computer code determines a ZL through individual cross-sections, then produces the following metrics: Negative Volume Displaced, Positive Volume Displaced, Net Volume Displaced, and Absolute Volume Displaced, along with a secondary set of metrics composed of six roughness parameters that allow definition of the ZL. From these metrics, a Zone of Interaction (ZOI) can be established.

This work was done by K. W. Street, Jr. of Glenn Research Center and R. L. Kobrick and D. M. Klaus of the University of Colorado – Boulder. Further information is contained in a TSP (see page 1).

Inquiries concerning rights for the commercial use of this invention should be addressed to NASA Glenn Research Center, Innovative Partnerships Office, Attn: Steven Fedor, Mail Stop 4–8, 21000 Brookpark Road, Cleveland, Ohio 44135. Refer to LEW-18675-1.

Detection of Carbon Monoxide Using Polymer-Carbon Composite Films

NASA's Jet Propulsion Laboratory, Pasadena, California

A carbon monoxide (CO) sensor was developed that can be incorporated into an existing sensing array architecture. The CO sensor is a low-power chemiresistor that operates at room temperature, and the sensor fabrication techniques are compatible with ceramic substrates.

Sensors made from four different polymers were tested: poly (4-vinylpyri-

dine), ethylene-propylene-diene-terpolymer, polyepichlorohydrin, and polyethylene oxide (PEO). The carbon black used for the composite films was Black Pearls 2000, a furnace black made by the Cabot Corporation. Polymers and carbon black were used as received. In fact, only two of these sensors showed a good response to CO. The poly (4-vinylpyridine) sensor is noisy, but it

does respond to the CO above 200 ppm. The polyepichlorohydrin sensor is less noisy and shows good response down to 100 ppm.

This work was done by Margie L. Homer, Margaret A. Ryan, and Liana M. Lara of Caltech for NASA's Jet Propulsion Laboratory. For more information, contact iaoffice@jpl.nasa.gov. NPO-47612

Substituted Quaternary Ammonium Salts Improve Low-Temperature Performance of Double-Layer Capacitors

Low cell resistances are observed when used with modified acetonitrile electrolyte blends.

NASA's Jet Propulsion Laboratory, Pasadena, California

Double-layer capacitors are unique energy storage devices, capable of supporting large current pulses as well as a very high number of charging and discharging cycles. The performance of double-layer capacitors is highly dependent on the nature of the electrolyte system used. Many applications, including for electric and fuel cell vehicles, back-up diesel generators, wind generator pitch control back-up power systems, environmental and structural distributed sensors, and

spacecraft avionics, can potentially benefit from the use of double-layer capacitors with lower equivalent series resistances (ESRs) over wider temperature limits. Higher ESRs result in decreased power output, which is a particular problem at lower temperatures. Commercially available cells are typically rated for operation down to only -40°C .

Previous briefs [for example, "Low Temperature Supercapacitors" (NPO-44386), *NASA Tech Briefs*, Vol. 32, No. 7

(July 2008), p. 32, and "Supercapacitor Electrolyte Solvents With Liquid Range Below -80°C " (NPO-44855), *NASA Tech Briefs*, Vol. 34, No. 1 (January 2010), p. 44] discussed the use of electrolytes that employed low-melting-point co-solvents to depress the freezing point of traditional acetonitrile-based electrolytes. Using these modified electrolyte formulations can extend the low-temperature operational limit of double-layer capacitors beyond that of commercially avail-

able cells. This previous work has shown that although the measured capacitance is relatively insensitive to temperature, the ESR can rise rapidly at low temperatures, due to decreased electrolyte conductance within the pores of the high-surface-area carbon electrodes. Most of these advanced electrolyte systems featured tetraethylammonium tetrafluoroborate (TEATFB) as the salt. More recent work at JPL indicates the use of the asymmetric quaternary ammonium salt triethylmethylammonium tetrafluoroborate (TEMATFB) or spiro-(1,1')-bipyrridolium tetrafluoroborate (SBPBF4) in a 1:1 by volume solvent mixture of acetonitrile (AN) and methyl formate (MF) enables double-layer capacitor cells to operate well below -40°C with a rela-

tively low ESR. Typically, a less than two-fold increase in ESR is observed at -65°C relative to room-temperature values, when these modified electrolyte blends are used in prototype cells. Double-layer capacitor coin cells filled with these electrolytes have displayed the lowest measured ESR for an organic electrolyte to date at low temperature (based on a wide range of electrolyte screening studies at JPL). The cells featured high-surface-area ($\approx 2,500\text{ m}^2/\text{g}$) carbon electrodes that were 0.50 mm thick and 1.6 cm in diameter, and coated with a thin layer of platinum to reduce cell resistance. A polyethylene separator was used to electrically isolate the electrodes.

This work was done by Erik J. Brandon, Marshall C. Smart, and William C. West of

Caltech for NASA's Jet Propulsion Laboratory. Further information is contained in a TSP (see page 1).

In accordance with Public Law 96-517, the contractor has elected to retain title to this invention. Inquiries concerning rights for its commercial use should be addressed to:

Innovative Technology Assets Management

JPL

Mail Stop 202-233

4800 Oak Grove Drive

Pasadena, CA 91109-8099

E-mail: iaoffice@jpl.nasa.gov

Refer to NPO-47327, volume and number of this NASA Tech Briefs issue, and the page number.

Sustainably Sourced, Thermally Resistant, Radiation Hard Biopolymer

A sustainably sourced biopolymer provides simultaneous thermal insulation and radiation protection.

Goddard Space Flight Center, Greenbelt, Maryland

This material represents a breakthrough in the production, manufacturing, and application of thermal protection system (TPS) materials and radiation shielding, as this represents the first effort to develop a non-metallic, non-ceramic, biomaterial-based, sustainable TPS with the capability to also act as radiation shielding. Until now, the standing philosophy for radiation shielding involved carrying the shielding at liftoff or utilizing onboard water sources. This shielding material could be grown onboard and applied as needed prior to different radiation landscapes (commonly seen during missions involving gravitational assists).

The material is a bioplastic material. Bioplastics are any combination of a biopolymer and a plasticizer. In this case, the biopolymer is a starch-based material and a commonly accessible plasticizer. Starch molecules are composed of two major polymers: amylose

and amylopectin.

The biopolymer phenolic compounds are common to the ablative thermal protection system family of materials. With similar constituents come similar chemical ablation processes, with the potential to have comparable, if not better, ablation characteristics. It can also be used as a flame-resistant barrier for commercial applications in buildings, homes, cars, and heater firewall material.

The biopolymer is observed to undergo chemical transformations (oxidative and structural degradation) at radiation doses that are 1,000 times the maximum dose of an unmanned mission (10–25 Mrad), indicating that it would be a viable candidate for robust radiation shielding. As a comparison, the total integrated radiation dose for a three-year manned mission to Mars is 0.1 krad, far below the radiation limit at which starch molecules degrade. For electron radiation, the biopolymer

starches show minimal deterioration when exposed to energies greater than 180 keV.

This flame-resistant, thermal-insulating material is non-hazardous and may be sustainably sourced. It poses no hazardous waste threats during its lifecycle. The material composition is radiation-tolerant up to megard doses, indicating its use as a radiation shielding material. It is lightweight, non-metallic, and able to be mechanically densified, permitting a tunable gradient of thermal and radiation protection as needed. The dual-use (thermal and radiation shielding), sustainable nature of this material makes it suitable for both industrial applications as a sustainable/green building material, and for space applications as thermal protection material and radiation shield.

This work was done by Diane Pugel of Goddard Space Flight Center. Further information is contained in a TSP (see page 1). GSC-16177-1



Integrated Lens Antennas for Multi-Pixel Receivers

This integrated lens antenna could enable high-resolution, three-dimensional imaging radar for homeland security applications.

NASA's Jet Propulsion Laboratory, Pasadena, California

Future astrophysics and planetary experiments are expected to require large focal plane arrays with thousands of detectors. Feedhorns have excellent performance, but their mass, size, fabrication challenges, and expense become prohibitive for very large focal plane arrays. Most planar antenna designs produce broad beam patterns, and therefore require additional elements for efficient coupling to the telescope optics, such as substrate lenses or micromachined horns.

An antenna array with integrated silicon microlenses that can be fabricated photolithographically effectively addresses these issues. This approach eliminates manual assembly of arrays of lenses and reduces assembly errors and tolerances. Moreover, an antenna array without metallic horns will reduce mass of any planetary instrument significantly.

The design has a monolithic array of lens-coupled, leaky-wave antennas operating in the millimeter- and submillimeter-wave frequencies. Electromagnetic simulations show that the electromagnetic

fields in such lens-coupled antennas are mostly confined in approximately 12–15°. This means that one needs to design a small-angle sector lens that is much easier to fabricate using standard lithographic techniques, instead of a full hyper-hemispherical lens. Moreover, this small-angle sector lens can be easily integrated with the antennas in an array for multi-pixel imager and receiver implementation. The leaky antenna is designed using double-slot irises and fed with TE₁₀ waveguide mode. The lens implementation starts with a silicon substrate. Photoresist with appropriate thickness (optimized for the lens size) is spun on the substrate and then reflowed to get the desired lens structure.

An antenna array integrated with individual lenses for higher directivity and excellent beam profile will go a long way in realizing multi-pixel arrays and imagers. This technology will enable a new generation of compact, low-mass, and highly efficient antenna arrays for use in multi-pixel receivers and imagers for future planetary and astronomical instru-

ments. These antenna arrays can also be used in radars and imagers for contra-band detection at stand-off distances.

This will be enabling technology for future balloon-borne, smaller explorer class mission (SMEX), and other missions, and for a wide range of proposed planetary sounders and radars for planetary bodies.

This work was done by Choonsup Lee and Goutam Chattopadhyay of Caltech and Nuria Llobart Juan for NASA's Jet Propulsion Laboratory. For more information, contact iaoffice@jpl.nasa.gov.

In accordance with Public Law 96-517, the contractor has elected to retain title to this invention. Inquiries concerning rights for its commercial use should be addressed to:

Innovative Technology Assets Management

JPL

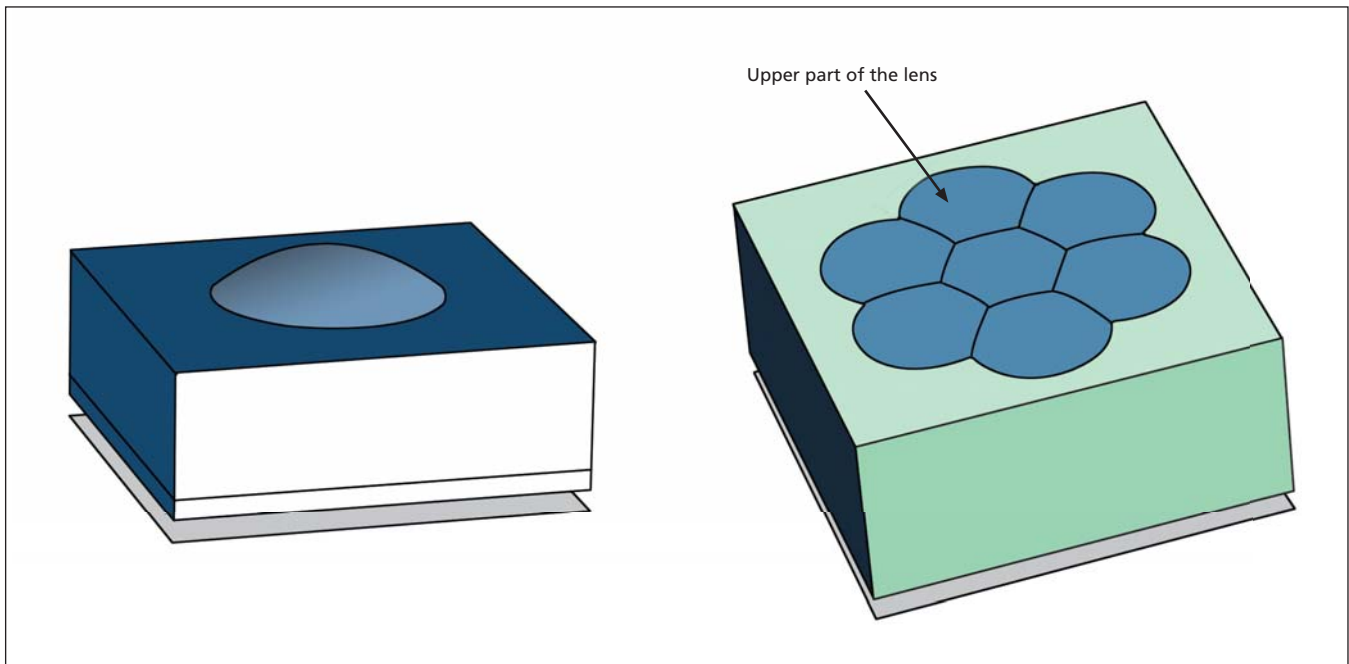
Mail Stop 202-233

4800 Oak Grove Drive

Pasadena, CA 91109-8099

E-mail: iaoffice@jpl.nasa.gov

Refer to NPO-46972, volume and number of this NASA Tech Briefs issue, and the page number.



The Dielectric Silicon Micro Lens (left) is shown with a possible array concept (right).

180-GHz Interferometric Imager

NASA's Jet Propulsion Laboratory, Pasadena, California

A 180-GHz interferometric imager uses compact receiver modules, combined high- and low-gain antennas, and ASIC (application specific integrated circuit) correlator technology, enabling continuous, all-weather observations of water vapor with 25-km resolution and 0.3-K noise in 15 minutes of observation for numerical weather forecasting and tropical storm prediction.

The GeoSTAR-II prototype instrument is broken down into four major subsystems: the compact, low-noise receivers; sub-array modules; IF signal distribution; and the digitizer/correlator. Instead of the single row of antennas adopted in GeoSTAR, this version has

four rows of antennas on a coarser grid. This dramatically improves the sensitivity in the desired field of view.

The GeoSTAR-II instrument is a 48-element, synthetic, thinned aperture radiometer operating at 165–183 GHz. The instrument has compact receivers integrated into “tiles” of 16 elements in a 4×4 arrangement. These tiles become the building block of larger arrays. The tiles contain signal distribution for bias controls, IF signal, and local oscillator signals. The IF signals are digitized and correlated using an ASIC correlator to minimize power consumption.

Previous synthetic aperture imagers have used comparatively large multichip

modules, whereas this approach uses chip-scale modules mounted on circuit boards, which are in turn mounted on the distribution manifolds. This minimizes the number of connectors and reduces system mass. The use of ASIC technology in the digitizers and correlators leads to a power reduction close to an order of magnitude.

This work was done by Pekka P. Kangaslahti, Boon H. Lim, Ian J. O'Dwyer, Mary M. Soria, Heather R. Owen, Todd C. Gaier, Bjorn H. Lambriksen, and Alan B. Tanner of Caltech, and Christopher Ruf of the University of Michigan for NASA's Jet Propulsion Laboratory. For more information, contact iaoffice@jpl.nasa.gov. NPO-47995

Maturation of Structural Health Management Systems for Solid Rocket Motors

Marshall Space Flight Center, Alabama

Concepts of an autonomous and automated space-compliant diagnostic system were developed for conditioned-based maintenance (CBM) of rocket motors for space exploration vehicles. The diagnostic system will provide real-time information on the integrity of critical structures on launch vehicles, improve their performance, and greatly increase crew safety while decreasing inspection costs. Using the SMART Layer technology as a basis, detailed procedures and calibration techniques for implementation of the diagnostic system were developed.

The diagnostic system is a distributed system, which consists of a sensor net-

work, local data loggers, and a host central processor. The system detects external impact to the structure. The major functions of the system include an estimate of impact location, estimate of impact force at impacted location, and estimate of the structure damage at impacted location.

This system consists of a large-area sensor network, dedicated multiple local data loggers with signal processing and data analysis software to allow for real-time, *in situ* monitoring, and long-term tracking of structural integrity of solid rocket motors. Specifically, the system could provide easy installation of

large sensor networks, onboard operation under harsh environments and loading, inspection of inaccessible areas without disassembly, detection of impact events and impact damage in real-time, and monitoring of a large area with local data processing to reduce wiring.

This work was done by Xinlin Qing, Shawn Beard, and Chang Zhang of Accellent Technologies, Inc for Marshall Space Flight Center. For more information, contact Sammy Nabors, MSFC Commercialization Assistance Lead, at sammy.a.nabors@nasa.gov. Refer to MFS-32819-1.

Validating Phasing and Geometry of Large Focal Plane Arrays CCD defects are used here to advantage.

NASA's Jet Propulsion Laboratory, Pasadena, California

The Kepler Mission is designed to survey our region of the Milky Way galaxy to discover hundreds of Earth-sized and smaller planets in or near the habitable zone. The Kepler photometer is an array of 42 CCDs (charge-coupled devices) in the focal plane of a 95-cm Schmidt camera onboard the Kepler spacecraft. Each 50×25-mm CCD has 2,200×1,024 pixels.

The CCDs accumulate photons and are read out every six seconds to prevent saturation. The data is integrated for 30 minutes, and then the pixel data is transferred to onboard storage. The data is subsequently encoded and transmitted to the ground.

During End-to-End Information System (EEIS) testing of the Kepler Mission

System (KMS), there was a need to verify that the pixels requested by the science team operationally were correctly collected, encoded, compressed, stored, and transmitted by the FS, and subsequently received, decoded, uncompressed, and displayed by the Ground Segment (GS) without the outputs of any CCD modules being flipped, mir-

rored, or otherwise corrupted during the extensive FS and GS processing. This would normally be done by projecting an image on the focal plane array (FPA), collecting the data in a flight-like way, and making a comparison between the original data and the data reconstructed by the science data system.

Projecting a focused image onto the FPA through the telescope would normally involve using a collimator suspended over the telescope opening. There were several problems with this approach: the collimation equipment is elaborate and expensive; as conceived, it could only illuminate a limited section of the FPA (≈ 25 percent) during a given test; the telescope cover would have to be deployed during testing to allow the image to be projected into the telescope; the equipment was bulky and difficult to situate in temperature-controlled environments; and given all the

above, test setup, execution, and repeatability were significant concerns. Instead of using this complicated approach of projecting an optical image on the FPA, the Kepler project developed a method using known defect features in the CCDs to verify proper collection and reassembly of the pixels, thereby avoiding the costs and risks of the optical projection approach.

The CCDs composing the Kepler FPA, as all CCDs, had minor defects. At ambient temperature, some pixels look far brighter than they should. These "hot" pixels have a higher rate of charge leakage than the others due to manufacturing variations. They are usually stable over time, and appear at temperatures above 5 °C. The hot pixels on the Kepler FPA were mapped before photometer assembly during module testing. Selected hot pixels were used as target "stars" for the purposes of EEIS testing. "Dead" pixels are

permanently off, producing a permanently black pixel. These can also be used if there is some illumination of the FPA.

During EEIS testing, Dark Current Full Frame Images (FFIs) taken at room temperature were used to create the hot pixel maps for all 84 Kepler photometer CCD channels. Data from two separate nights were used to create two hot pixel maps per channel, which were cross-correlated to remove cosmic ray events which appear to be hot pixels. These hot pixel maps obtained during EEIS testing were compared to the maps made during module testing to verify that the end-to-end data flow was correct.

This work was done by Shaun P. Standley and Thomas N. Gautier of Caltech; Douglas A. Caldwell of SETI Institute; and Maura Rabbette of Ames Research Center for NASA's Jet Propulsion Laboratory. For more information, contact iaoffice@jpl.nasa.gov. NPO-46868

Transverse Pupil Shifts for Adaptive Optics Non-Common Path Calibration

NASA's Jet Propulsion Laboratory, Pasadena, California

A simple new way of obtaining absolute wavefront measurements with a laboratory Fizeau interferometer was recently devised. In that case, the observed wavefront map is the difference of two cavity surfaces, those of the mirror under test and of an unknown reference surface on the Fizeau's transmission flat. The absolute surface of each can be determined by applying standard wavefront reconstruction techniques to two grids of absolute surface height differences of the mirror under test, obtained from pairs of measurements made with slight transverse shifts in X and Y.

Adaptive optics systems typically provide an actuated periscope between wavefront sensor (WFS) and common-mode optics, used for lateral registration of deformable mirror (DM) to WFS. This periscope permits independent adjustment of either pupil or focal spot incident on the WFS. It would be used to give the required lateral pupil motion between common and non-common segments, analogous to the lateral shifts of the two phase contributions in the lab Fizeau.

The technique is based on a completely new approach to calibration of

phase. It offers unusual flexibility with regard to the transverse spatial frequency scales probed, and will give results quite quickly, making use of no auxiliary equipment other than that built into the adaptive optics system. The new technique may be applied to provide novel calibration information about other optical systems in which the beam may be shifted transversely in a controlled way.

This work was done by Eric E. Bloemhof of Caltech for NASA's Jet Propulsion Laboratory. Further information is contained in a TSP (see page 1). NPO-48060

Qualification of Fiber Optic Cables for Martian Extreme Temperature Environments

NASA's Jet Propulsion Laboratory, Pasadena, California

Means have been developed for enabling fiber optic cables of the Laser Induced Breakdown Spectrometer instrument to survive ground operations plus the nominal 670 Martian conditions that include Martian summer and winter seasons. The purpose of this development was to validate the use of the rover exter-

nal fiber optic cabling of ChemCam for space applications under the extreme thermal environments to be encountered during the Mars Science Laboratory (MSL) mission.

Flight-representative fiber optic cables were subjected to extreme temperature thermal cycling of the same diur-

nal depth (or ΔT) as expected in flight, but for three times the expected number of in-flight thermal cycles. The survivability of fiber optic cables was tested for 600 cumulative thermal cycles from -130 to $+15$ °C to cover the winter season, and another 1,410 cumulative cycles from -105 to $+40$ °C to cover the

summer season. This test satisfies the required 3 times the design margin that is a total of 2,010 thermal cycles (670×3). This development test included functional optical transmission tests during the course of the test. Transmission of the fiber optic cables was per-

formed prior to and after 1,288 thermal cycles and 2,010 thermal cycles. No significant changes in transmission were observed on either of the two representative fiber cables subject through the 3X MSL mission life that is 2,010 thermal cycles.

This work was done by Rajeshuni Ramesham, Christian A. Lindensmith, William T. Roberts, and Richard A. Rainen of Caltech for NASA's Jet Propulsion Laboratory. For more information, contact iaoffice@jpl.nasa.gov. NPO-48055

Solid-State Spectral Light Source System

Goddard Space Flight Center, Greenbelt, Maryland

A solid-state light source combines an array of light-emitting diodes (LEDs) with advanced electronic control and stabilization over both the spectrum and overall level of the light output. The use of LEDs provides efficient operation over a wide range of wavelengths and power levels, while electronic control permits extremely

stable output and dynamic control over the output.

In this innovation, LEDs are used instead of incandescent bulbs. Optical feedback and digital control are used to monitor and regulate the output of each LED. Because individual LEDs generate light within narrower ranges of wavelengths than incandescent bulbs, multiple LEDs

are combined to provide a broad, continuous spectrum, or to produce light within discrete wavebands that are suitable for specific radiometric sensors.

This work was done by Robert Maffione and David Dana of Hydro-Optics, Biology & Instrumentation Laboratories, Inc. for Goddard Space Flight Center. Further information is contained in a TSP (see page 1). GSC-15851-1

Multiple-Event, Single-Photon Counting Imaging Sensor

This sensor has applications in high-energy physics and medical and biological imaging systems.

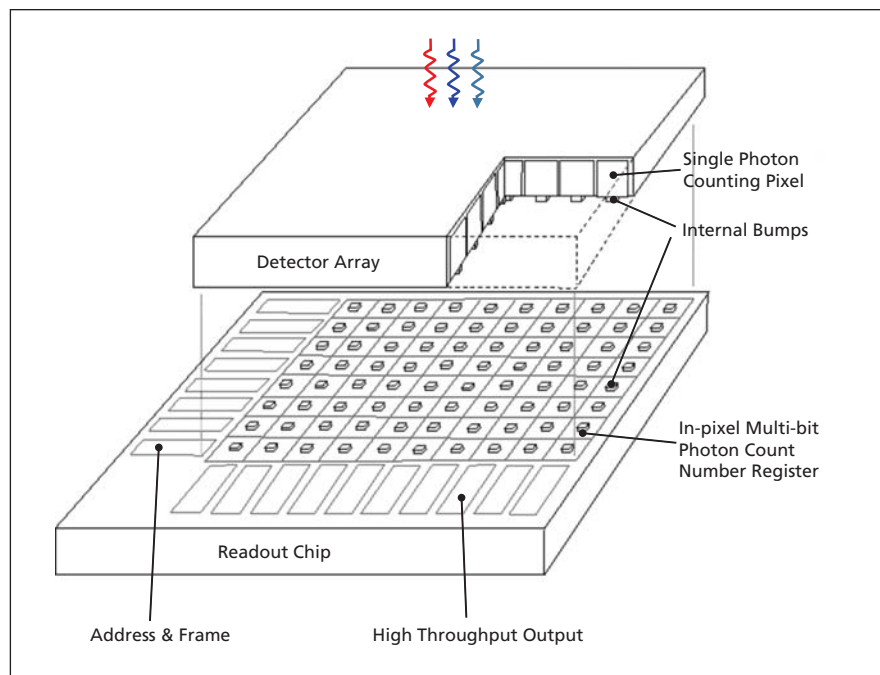
NASA's Jet Propulsion Laboratory, Pasadena, California

The single-photon counting imaging sensor is typically an array of silicon Geiger-mode avalanche photodiodes that are monolithically integrated with CMOS (complementary metal oxide semiconductor) readout, signal processing, and addressing circuits located in each pixel and the peripheral area of the chip. The major problem is its "single-event" method for photon count number registration. A single-event single-photon counting imaging array only allows registration of up to one photon count in each of its pixels during a frame time, i.e., the interval between two successive pixel reset operations. Since the frame time can't be too short, this will lead to very low dynamic range and make the sensor merely useful for very low flux environments. The second problem of the prior technique is a limited fill factor resulting from consumption of chip area by the monolithically integrated CMOS readout in pixels. The resulting low photon collection efficiency will substantially ruin any benefit gained from the very sensitive single-photon counting detection.

The single-photon counting imaging sensor developed in this work has a novel "multiple-event" architecture, which allows each of its pixels to register

as more than one million (or more) photon-counting events during a frame time. Because of a consequently boosted dynamic range, the imaging array of the invention is capable of performing sin-

gle-photon counting under ultra-low light through high-flux environments. On the other hand, since the multiple-event architecture is implemented in a hybrid structure, back-illumination and



Structure of a multiple-event **Single-Photon Counting Imaging Sensor** implemented using flip-chip bump bonding technique.

close-to-unity fill factor can be realized, and maximized quantum efficiency can also be achieved in the detector array.

A multiple-event single-photon counting imaging sensor consists of a readout chip and a single-photon counting detector array (see figure) integrated in stack using flip-chip bump bonding, direct wafer bonding, or other 3D integration technologies. Supported by the state-of-the-art CMOS technology, each of the readout pixels can contain several hundred transistors in the area of the pixel. These transistors can compose a 20-bit digital counter, a related latch of the same bits, an active quenching circuit consisting of a delay inverter and a reset circuit, and an exposure control circuit for registration of up to one million photon counts during a frame time.

The architecture will be slightly changed if a self-quenching single-photon counting detector array is used, where the external quenching circuit of the readout circuit is replaced by a simple MOSFET (metal-oxide semiconductor field-effect transistor) load. As a re-

sult of the substantial change of treatable photon-counting number during a frame time from one of the prior art to 10^6 of the invention, the dynamic range of the imaging sensor will increase by 120 dB. Hence, a multiple-event single-photon counting imaging sensor can attain an unprecedentedly high dynamic range of around 160–180 dB. The resulting dynamic range has excellent linearity through its whole range. Unlike the prior high dynamic range techniques that rely on logarithmic operation on analog signal and have exponentially decayed grayscale resolution towards high light level, the multiple-event single-photon imaging sensor will show high and uniform grayscale resolution through the whole dynamic range. Subtle grayscale variation at even very high light levels, e.g., the contrast of a bright object and a slightly brighter object in one scene, can be distinguished by this unique capability.

Separation of the detector array from the readout chip makes it possible for the detector array to attain maximized

photon collection efficiency. Photon collection efficiency is mainly the product of fill factor and quantum efficiency of the detector. The detector array of the multiple-event single-photon counting imaging sensor has a back-illuminated structure and a near 100-percent fill factor. The absorption layer of the detector can be tuned within a wide range of thicknesses to maximize the quantum efficiency for the interested wavelength.

While the readout chip is implemented using silicon CMOS technology, the single-photon counting detector array can be built on silicon or other semiconductor materials such as InGaAs/InP, HgCdTe (MCT), or GaN/GaAlN. With such flexibility, this technique can cover a wide range of wavelengths from the ultraviolet through mid-infrared.

This work was done by Xinyu Zheng, Thomas J. Cunningham, and Chao Sun of Caltech; and Kang L. Wang of UCLA for NASA's Jet Propulsion Laboratory. Further information is contained in a TSP (see page 1). NPO-45747



Books & Reports

Surface Modeling to Support Small-Body Spacecraft Exploration and Proximity Operations

In order to simulate physically plausible surfaces that represent geologically evolved surfaces, demonstrating demanding surface-relative guidance navigation and control (GN&C) actions, such surfaces must be made to mimic the geological processes themselves. A report describes how, using software and algorithms to model body surfaces as a series of digital terrain maps, a series of processes was put in place that evolve the surface from some assumed nominal starting condition.

The physical processes modeled in this algorithmic technique include fractal regolith substrate texturing, fractally textured rocks (of empirically derived size and distribution power laws), cratering, and regolith migration under potential energy gradient. Starting with a global model that may be determined observationally or created *ad hoc*, the surface evolution is begun. First, material of some assumed strength is layered on the global model in a fractally random pattern. Then, rocks are distributed according to power laws measured on the Moon. Cratering then takes place in a temporal fashion, including model-

ing of ejecta blankets and taking into account the gravity of the object (which determines how much of the ejecta blanket falls back to the surface), and causing the observed phenomena of older craters being progressively buried by the ejecta of earlier impacts. Finally, regolith migration occurs which stratifies finer materials from coarser, as the fine material progressively migrates to regions of lower potential energy.

This work was done by Joseph E. Riedel and Nickolaos Mastrodemos of Caltech and Robert W. Gaskell of the Planetary Science Institute for NASA's Jet Propulsion Laboratory. Further information is contained in a TSP (see page 1). NPO-47233

Achieving Exact and Constant Turnaround Ratio in a DDS-Based Coherent Transponder

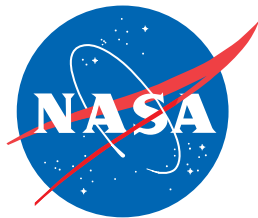
A report describes a non-standard direct digital synthesizer (DDS) implementation that can be used as part of a coherent transponder so as to allow any rational turnaround ratio to be exactly achieved and maintained while the received frequency varies. (A coherent transponder is a receiver-transmitter in which the transmitted carrier is locked to a pre-determined multiple of the received carrier's frequency and

phase. That multiple is called the turnaround ratio.)

The report also describes a general model for coherent transponders that are partly digital. A partially digital transponder is one in which analog signal processing is used to convert the signals between high frequencies at which they are radiated and relatively low frequencies at which they are converted to or from digital form, with most of the complex processing performed digitally. There is a variety of possible architectures for such a transponder, and different ones can be selected by choosing different parameter values in the general model.

Such a transponder uses a DDS to create a low-frequency quasi-sinusoidal signal that tracks the received carrier's phase, and another DDS to generate an IF or near-baseband version of the transmitted carrier. With conventional DDS implementations, a given turnaround ratio can be achieved only approximately, and the error varies slightly as the received frequency changes. The non-conventional implementation employed here allows any rational turnaround ratio to be exactly maintained.

This work was done by Larry R. D'Addario of Caltech for NASA's Jet Propulsion Laboratory. Further information is contained in a TSP (see page 1). NPO-47460



National Aeronautics and
Space Administration